ASPS Conference Proceedings 1: 1241-1245 (2022)

Proceedings of

12th Structural Engineering Convention-An International Event (SEC 2022)

Available at https://asps-journals.com/index.php/acp

Blast Resistance Capacity of Seismically Designed Building Frames

S. Tolani [1,*] , S. D. Bharti [2], M. K. Shrimali [3], T. K. Datta [4]

[1] Department of Civil Engineering, Assistant Professor, Swami Keshvanand Institute of Technology, M&G, Jaipur, 302 017, India
[2] National Center for Disaster Mitigation and Management, Professor, Malaviya National Institute of Technology, Jaipur, 302 017, India
[3] National Center for Disaster Mitigation and Management, Professor, Malaviya National Institute of Technology, Jaipur, 302 017, India
[4] Department of Civil Engineering, Emeritus Professor, Indian Institute of Technology, Delhi, New Delhi, India

Paper ID - 090345

Abstract

Because of the inherent uncertainty in the blast loading caused due to terrorist attacks, most buildings are not designed for blast loading, but they are routinely designed for earthquake demand. If the blast resistance capacity of the seismically designed building can be evaluated, the risk of the blast loading caused due to the terrorist attacks can be reduced by upgrading the seismic design of the building. With this background in view, the present paper investigates the blast resistance capacity of a 6 storey building frame designed for extreme peak ground acceleration (PGA) levels of 0.5g, 0.4g, and 0.3g. The 3D model of the 6 storey building is designed according to Indian Standard (IS) codes for the above mentioned extreme level earthquake. Designed buildings are subjected to surface blast of 500 kg of TNT(trinitrotoluene) at different standoff distances ranging from 5m to 30m. The time histories of the blast loading due to air pressure and ground shock are modeled by those existing literature. A nonlinear time history of analysis (NTHA) of the frame is performed in SAP 2000 for surface blast and the simulated earthquakes from the specified response spectrum in IS code. NTHA results for both cases are compared to evaluate the relative performance of the three different seismically designed buildings to the surface blast loading. The response quantities of interest include maximum drift, maximum top displacement, and number of hinges formed. The results of the study indicate that for the near blast conditions the blast resistance capacity of the building increases with the increase in the PGA values for which the building is designed. By upgrading the seismic design by 0.1g, the blast resistance capacity increases manifold for near blast conditions. Thus, by updating the seismic design of a building, the risk of blast loading in the design may be considerably mitigated.

Keywords: Surface blast, RC building, Nonlinear Time History Analysis

1. Introduction

In the recent past, important buildings have become a common target of terrorists as it causes both financial loss and a large number of casualties. In such cases, a major part of the casualties is caused due to the structural damage. Some guidelines are available [1–4], which provide empirical charts and equations to calculate blast load on structures and design recommendations. Also, different guidelines are published for reducing the risk of progressive collapse of structures [5–7]. Despite this, blast loading is rarely taken into account in the design of buildings because there are a large number of uncertainties involved with this load. The location of the blast source and its intensity are always uncertain and also, consideration of blast loading in design will be very uneconomic. So, the conventional design process involves earthquake and wind loads only.

Blast and earthquake load are different. The blast load is of shorter duration and higher magnitude than the earthquake load. But, the design of structure for both loads involves providing sufficient strength and ductility to resist these loads. Some researchers examined the blast resistance capacity of earthquake-resistant buildings [8,9]. Draganic and Sigmund [8] found that conventional reinforcement in elements provides adequate ductility when these elements are subjected to distant explosions, while for near blast condition additional reinforcement needs to be provided. Kyei and Abass [9] studied the effect of blast loading on seismically detailed RC columns and concluded that by reducing the spacing of transverse reinforcement in columns, lateral displacement can be reduced for near blast conditions. Thus, the structure which is designed for earthquake loading may resist blast load also to some extent. Therefore, the blast resistance capacity of a building designed for different levels of earthquake intensities should be properly evaluated in order to reduce risk of the blast loading by upgrading the seismic design of the building.

The literature on the effect of aboveground blast on structures mostly considers air pressure effect on structures [10–12], whereas, a surface explosion exerts both air pressure and ground shock effect on the nearby structure. There is very little literature available on surface blast effect with consideration of both ground shock and air pressure effect on structures. Wu and Hao [13] developed empirical equations to predict air pressure and ground acceleration produced by a

*Corresponding author. Tel: +919910938238; E-mail address: sunitatolani1@gmail.com

Published online: December 19, 2022
doi:10.38208/acp.v1.647

surface blast and investigated the effect of these two forces on a single storey masonry infilled RC building [14].

The present study investigates the blast resistance capacity of a 6 storey RC building designed for different PGA levels of 0.5g, 0.4g, and 0.3g. The 3D model of the 6 storey building is designed according to Indian Standard (IS) codes for the above mentioned extreme level earthquake. Designed buildings are subjected to surface blast of 500 kg of TNT(trinitrotoluene) at 5m, 10m, 15m, and 30m standoff distances. A nonlinear time history of analysis (NTHA) of the frame is performed in SAP 2000 for surface blast and the simulated earthquakes from the specified response spectrum in IS code. The behavior of the building is evaluated in terms of the response quantities, which include peak story displacements, the maximum inter-story drifts, and the number of plastic hinges formed.

2. Theory

2.1 Blast Loading

The behavior of the building is investigated for the surface blast. A surface blast generates both air pressure and ground vibration effect on a nearby structure as shown in Fig. 1. To simulate the effect of the surface blast, the air pressure time history is applied on the exposed surface of the building and the ground acceleration time history is applied at the base of the building. The air pressure time history and ground acceleration time history are generated with the help of empirical formulae developed by Wu and Hao [13]. These expressions are generated in the form of standoff distance and charge weight. The expressions are given below.

Air Pressure

Peak pressure in free air from the surface explosion is given by (Wu and Hao 2005):

$$p_{so} = 1.059\left(\frac{R}{Q^{1/3}}\right)^{-2.56} - 0.051,\ 0.1 \le R/Q^{1/3} \le 1 \text{(MPa)} \quad (1)$$

$$p_{so} = 1.008\left(\frac{R}{Q^{1/3}}\right)^{-2.01},\ 10 \ge R/Q^{1/3} > 1 \text{ (MPa)} \quad (2)$$

where R is distance in meters measured from the charge centre and Q is the TNT equivalent charge weight in kilograms.

Peak reflected air pressure along the height of the front wall of the structure is given by:

$$p_r(h) = p_{ro}(1 - 0.0006 p_{ro}^{0.46} h^2),\ p_{ro} \le 10 \text{ MPa} \quad (3)$$

where h is the wall height in meters and p_{ro} is the peak reflected pressure at the bottom of the wall, which is estimated by:

$$p_{ro} = 2.85(p_{so})^{1.206},\ p_{so} \le 50 \text{ MPa} \quad (4)$$

The shock wave front arrival time is given by:

$$T_a = 0.34 R^{1.4} Q^{-0.2} / c_a \quad \text{(sec)} \quad (5)$$

where c_a is the sound speed in air.

The pressure time history is assumed as increasing linearly from zero to peak value with a rising time T_r, and then decreasing exponentially with decreasing time T_d (Figure 1b), the total duration of positive pressure is given by

$$T_+ = T_r + T_d \quad (6)$$

$$T_r = 0.0019(R/Q^{1/3})^{1.30} \quad \text{(sec)} \quad (7)$$

$$T_d = 0.0005 R^{0.72} Q^{0.16} \quad \text{(sec)} \quad (8)$$

The linear part of air pressure time history for the pressure rising from zero to its peak value is

$$p_s(t) = p_{so}\left(\frac{t}{T_r}\right),\ 0 \le t \le T_r, \quad (9)$$

The exponential decay phase is

$$p_s(t) = p_{so}\left(1 - \frac{t - T_r}{T_d}\right)\exp\left(-\frac{a(t - T_r)}{T_d}\right),\ Tr \le t \quad (10)$$

$$a = \begin{cases} 3.02 p_{so}^{0.38} + 6.85 p_{so}^{0.79} \exp\left(-4.55\dfrac{t - T_r}{T_d}\right), T_r \le t \le T_+ \\ 1.96 p_{so}^{0.25} + 0.176 p_{so} \exp\left(-0.73 p_{so}^{-0.49} \dfrac{t - T_+}{T_d}\right), T_+ < t \end{cases} \quad (11)$$

Ground Shock

These equations are simulated from a one-ton surface explosion at different distances at a granite site. For the granite site, the PPA (peak particle acceleration) was predicted as (Wu and Hao 2005)

$$PPA = 3.979 R^{-1.45} Q^{1.07},\ \text{(g)} \quad (12)$$

The arrival time at a point on the ground surface

$$t_a = 0.91 R^{1.03} Q^{-0.02} / c_s,\ \text{(sec)} \quad (13)$$

Where c_s is the P wave velocity of the granite site.

The duration of the acceleration time history is

$$t_d = 0.0045 R^{0.45},\ \text{(sec)} \quad (14)$$

And its principal frequency can be estimated by

$$\text{PF} = 465.62(R/Q^{1/3})^{-0.13},\ 0.3 \le R/Q^{1/3} \le 10,\ \text{(Hz)} \quad (15)$$

The power spectrum of acceleration time history can be represented by a Tazimi-Kanai function

$$S(f) = \frac{1 + 4\zeta_g^2 (f^2/\text{PF}^2)}{(1 - f^2/\text{PF}^2)^2 + 4\zeta_g^2 (f^2/\text{PF}^2)} S_0, \quad (16)$$

(c)

where ζ_g is a parameter governing the power spectral shape, S_0 is the amplitude of power spectrum of a white noise or a scaling factor of the spectrum. The sample time histories of ground shock are generated using Monte-Carlo simulation and the simulated time histories are multiplied by the shape function. The shape function of a simulated acceleration time history is given by

$$\begin{cases} 0 & t \le 0 \\ mte^{-nt^2} & t > 0 \end{cases} \tag{17}$$

where m and n are parameters related to ground motion non-stationarity.

Earthquake Loading

Artificial time histories compatible with IS 1893, 2002 Response spectrum are generated for design basis earthquake (DBE) and maximum considered earthquakes (MCE). For generating the artificial time histories from the response spectrum of the earthquake, the Seismosignal software is used.

3. Numerical Study

A 6-storey building is considered for investigation. Plan dimensions of the building are 24m X 24m with four equal spans in each direction and the height of each storey is 3m. Grade of concrete is M30 and the grade of steel bars is Fe 415. The 3D model of the building frame (Fig. 1) is designed for gravity load and three extreme PGA levels. The 3D frames named Frame-A, Frame-B, and Frame-C (Table 1) are designed for PGA levels of 0.3g, 0.4g, and 0.5g respectively. Properties of the three building frames are shown in Table 1.

The position of the surface blast is shown in Fig.1. The charge weight (Q) is assumed to be 500kg of TNT acting at standoff distances (R) 5m, 10m, 15m, 30m, and the structural response to explosive loads at different distances are simulated in the analysis. Fig. 2 shows simulated air pressure time history applied to the bottom storey of the building and ground acceleration time history. The shape of the air pressure time history applied to the upper storeys is the same but, the magnitude of the peak pressure and time of arrival of the air pressure wave are different as obtained by the equations 1-11. The nonlinear time history analysis of the frame is carried out for both blast loading and earthquake loading using SAP 2000.

4. Results and discussions

The building frames designed for three different PGA levels are subjected to blast loading produced by the explosion of 500kg of TNT on the ground surface at standoff distances 5m, 10m, 15m and 30m from the building. The effect of the PGA level for which the building is designed on the blast resistance capacity of the building is investigated. The response of the building frames for response spectrum compatible time histories of ground motion with design level (0.2g) and extreme level (0.4g) earthquakes is also evaluated. Responses of the buildings are obtained in terms of top floor displacement, inter-storey drift, and number of plastic hinges formed.

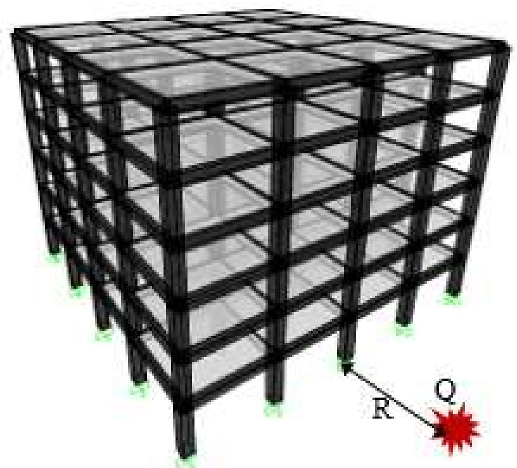

Fig. 1. 3D view of the building frame

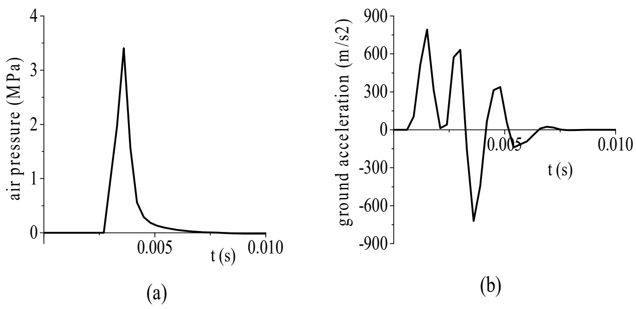

Fig. 2. (a) air pressure time history (b) ground acceleration time history for surface explosion of 500kg of TNT at 5m standoff distance

Table 1. Properties of the building frames.

	Frame-A	Frame-B	Frame-C
Column Size (mm)	550x550	650x650	750x750
Column R/F (%)	1.3	1.4	1.5
Beam Size (mm)	300x550	300x550	350x600
Beam R/F (%)	1.2 (top) 0.6 (bottom)	1.6 (top) 0.8 (bottom)	1.6 (top) 0.8 (bottom)
Slab Size (mm)	200	200	200
T_1(s)	0.97	0.88	0.74
T_2 (s)	0.31	0.27	0.22

Fig. 3 shows top floor displacement time history plots for surface blast load. It is seen from the figure that for the surface blast of 500kg TNT at 5m standoff distance, the Frame-A is collapsed at 0.5 s, whereas Frame -B and Frame-C exhibited large top floor displacement but not collapsed. The maximum top floor displacement of Frame-B is 30% more than that of Frame-C. Further, we can see that the maximum top floor displacement of the three frames for 10m standoff distance is 60% less than that for 5m standoff distance, and for 15m standoff distance, it is 32% less than that for 10m standoff distance. Therefore, the response of structure reduces rapidly with standoff distance for near blast condition, and for a distant blast, this reduction is less.

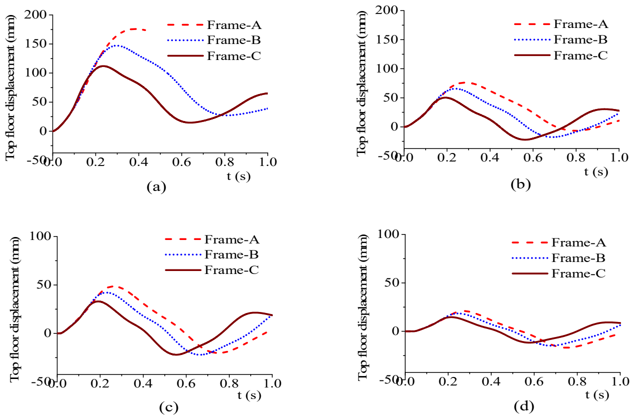

Fig. 3. Top floor displacement time history plots due to surface blast of 500kg TNT at standoff distance (a) 5m (b) 10m (c) 15m (d) 30m

Fig. 4 shows plots of maximum top floor displacement and maximum drift of the three frames for different values of standoff distance. It can be seen that at 5m standoff distance, the maximum value of top floor displacement for Frame-A is 20% more than that for Frame-B which is 30% more than Frame-C. This difference is reducing with an increase in standoff distance, for 30m standoff distance, this difference reduces to 10-11%. Similarly, the maximum drift of Frame-A at 5m standoff distance is 40% more than that for Frame-B and this value for Frame-B is 33% more than the maximum drift value of Frame-C. At 30m standoff distance, this difference reduces to only 8-9%. It indicates that upgrading the seismic design of a building increases its blast resistance capacity for near blast conditions, whereas, for the distant blast conditions, the effect of this up-gradation is less.

Fig. 5 shows top floor displacement plots for earthquake loading. It can be seen from figures that there is a considerable difference in the response of the three frames for extreme level earthquake but for design basis earthquake this difference is less. Table 1 shows the maximum values of top floor displacement and inter-storey drift of the three frames for both types of earthquakes. It can be seen that for DBE, the response of Frame-B is almost 10% less than that of Frame-A. A similar amount of difference is there between responses of Frame-B and Frame-C. But for MCE, this difference is about 25%.

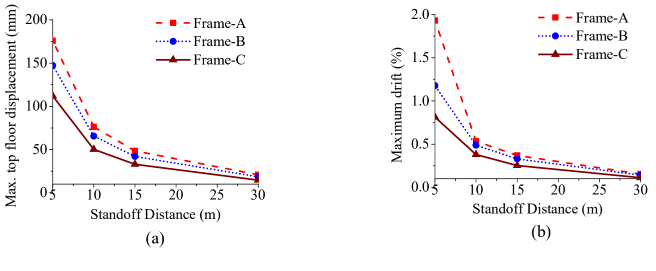

Fig. 4. (a) Maximum top floor displacement (b) Maximum inter-storey drift due to surface blast

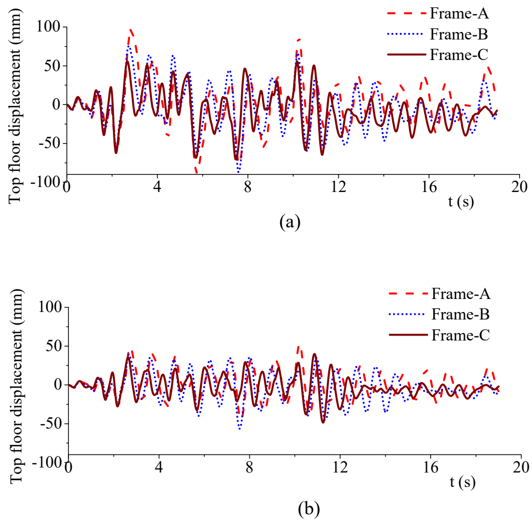

Fig. 5. Top floor displacement time history plots due to earthquake response spectrum compatible time history for (a) MCE-0.4g (b) DBE-0.2g

Table 2. Response of the building frames for earthquake load

	DBE (0.2g)		MCE (0.4g)	
	Max. top floor disp.(mm)	Max. drift (%)	Max. top floor disp. (mm)	Max. drift (%)
Frame-A	56	0.44	96	0.82
Frame-B	52	0.42	87	0.66
Frame-C	48	0.38	70	0.52

Fig. 6 shows the number of hinges formed for both blast load and earthquake load. It was observed that the Frame-A is collapsed at 0.5s due to the formation of a large number of hinges due to 500kg blast at 5m standoff distance (scaled distance $R/Q^{1/3}$ =0.6). Frame-B and Frame-C were damaged but not collapsed. With the increase in standoff distance, number of hinges is reducing by a considerable amount. At standoff distance 30m (scaled distance $R/Q^{1/3}$=3.7) no hinges are formed in Frame-C, its response is within the elastic limit. A little number of hinges are formed in Frame-B and there is some damage in Frame-A. Similarly, for earthquake loading difference between the number of hinges formed in the three frames is more for the MCE level earthquake than that for the DBE level earthquake.

Also, due to DBE (0.2g) level earthquake, hinges are formed in the building frames designed for PGA 0.3g, 0.4g, and 0.5g because as per the code these buildings are designed for forces which are 5 times less than the considered PGA level (Response reduction factor R=5).

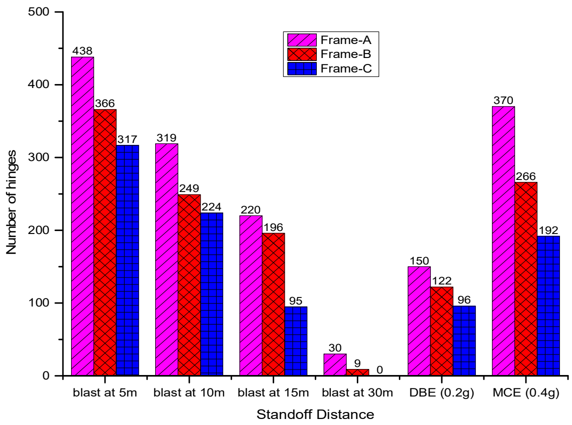

Fig. 6. Number of hinges formed due to surface blast and earthquake load

5. Conclusions

The performance of three seismically designed building frames under the surface blast effect is evaluated. Also, the response of the buildings under the response spectrum compatible earthquake time histories is investigated. Response quantities of interest are top floor displacement, drift, and number of hinges formed. Following conclusions are obtained from the study:

1. Responses of the building sharply fall with standoff distance in the close vicinity of the structure (R≤10m), thereafter the responses continue to decrease very mildly with R.
2. By upgrading the seismic design by 0.1g, the blast resistance capacity increases manifold for near blast conditions, the maximum effect is observed on the inter-storey drift of the buildings.
3. For distant blast conditions, the top floor displacement and inter-storey drift of the building frames designed for different PGA levels remain almost the same.
4. For the MCE level (0.4g) earthquake, upgradation of seismic design plays a significant role on the performance of the building, whereas this effect is less for DBE (0.2g) level earthquake.
5. For this particular problem, the building designed for PGA level 0.3g is collapsed due to surface blast of 0.6 scaled distance and suffered some damage for the scaled distance 3.7.
6. The building designed for PGA level 0.5g suffered considerable damage due to surface blast of 0.6 scaled distance but not collapsed whereas it remained within elastic range for the scaled distance 3.7.

Disclosures

Free Access to this article is sponsored by SARL ALPHA CRISTO INDUSTRIAL.

References

[1] DoD. Structures to Resist the Effects of Accidental Explosions, 2008.

[2] CEN. Eurocode 1 - Actions on structures - Part 1-7: General actions - Accidental actions Eurocode, 2006.

[3] IS 4991. Criteria for Blast Resistant Design of Structures for Eeplosions Above Ground. Bureau of Indian Standards; 2003.

[4] FEMA 426. Building Terrorism Mitigation - Blast and CBR Measures. 2003.

[5] DoD. Design of buildings to resist progressive collapse, 2016.

[6] GSA. Progressive collapse analysis and design guidelines for new federal office buildings and major modernization projects., 2003. doi:10.1061/40700(2004)156.

[7] NISTIR. Best practices for reducing the potential for progressive collapse in buildings, 2007.

[8] Draganić H, Sigmund V. Blast loading on structures. Technical Gazette 2012;19:643–52.

[9] Kyei C, Braimah A. Effects of transverse reinforcement spacing on the response of reinforced concrete columns subjected to blast loading. Engineering Structures 2017;142:148–64. doi:10.1016/j.engstruct.2017.03.044.

[10] Ali MM. Protective design of concrete buildings under blast loading. Structures under Shock and Impact VII 2002;11:23–33.

[11] Goel MD, Matsagar VA, Gupta AK, Marburg S. An abridged review of blast wave parameters. Defence Science Journal 2012;62:300–6. doi:10.14429/dsj.62.1149.

[12] Jayasooriya R. Vulnerability and Damage Analysis of Reinforced Concrete Framed Buildings. 2010.

[13] Wu C, Hao H. Modeling of simultaneous ground shock and airblast pressure on nearby structures from surface explosions. International Journal of Impact Engineering 2005;31:699–717. doi:10.1016/j.ijimpeng.2004.03.002.

[14] Wu C, Hao H. Numerical simulation of structural response and damage to simultaneous ground shock and airblast loads. International Journal of Impact Engineering 2007;34:556–72. doi:10.1016/j.ijimpeng.2005.11.003.